Remote Sensing of Environment 169 (2015) 139–149

Contents lists available at ScienceDirect

Remote Sensing of Environment

journal homepage: www.elsevier.com/locate/rse

Secchi disk depth: A new theory and mechanistic model for underwater visibility

ZhongPing Lee [a,*], Shaoling Shang [b,*], Chuanmin Hu [c], Keping Du [d], Alan Weidemann [e], Weilin Hou [e], Junfang Lin [a], Gong Lin [b]

[a] School for the Environment, University of Massachusetts Boston, Boston, MA 02125, United States
[b] State Key Laboratory of Marine Environmental Science, Xiamen University, Xiamen 361005, China
[c] College of Marine Science, University of South Florida, St. Petersburg, FL 33701, United States
[d] State Key Laboratory of Remote Sensing Science, Beijing Normal University, Beijing 100875, China
[e] Naval Research Laboratory, Stennis Space Center, MS 39529, United States

ARTICLE INFO

Article history:
Received 16 April 2015
Received in revised form 3 August 2015
Accepted 4 August 2015
Available online xxxx

Keywords:
Secchi disk depth
Water transparency
Visibility theory
Remote sensing
Beam attenuation coefficient
Diffuse attenuation coefficient

ABSTRACT

Secchi disk depth (Z_{SD}) is a measure of water transparency, whose interpretation has wide applications from diver visibility to studies of climate change. This transparency has been explained in the past 60 + years with the underwater visibility theory, the branch of the general visibility theory for visual ranging in water. However, through a thorough review of the physical processes involved in visual ranging in water, we show that this theory may not exactly represent the sighting of a Secchi disk by a human eye. Further, we update the Law of Contrast Reduction, a key concept in visibility theory, and develop a new theoretical model to interpret Z_{SD}. Unlike the classical model that relies strongly on the beam attenuation coefficient, the new model relies only on the diffuse attenuation coefficient at a wavelength corresponding to the maximum transparency for such interpretations. This model is subsequently validated using a large (N = 338) dataset of independent measurements covering oceanic, coastal, and lake waters, with results showing excellent agreement (~18% average absolute difference, $R^2 = 0.96$) between measured and theoretically predicted Z_{SD} ranging from <1 m to >30 m without regional tuning of any model parameters. This study provides a more generalized view of visual ranging, and the mechanistic model is expected to significantly improve the current capacity in monitoring water transparency of the global aquatic environments via satellite remote sensing.

1. Introduction

Secchi disk, a white or black-and-white disk with a diameter generally about 30 cm, is the oldest "optical instrument" used to measure transparency of ocean and lake waters (see Tyler (1968), Wernand (2010), and Aas, Høkedal, and Sørensen (2014) for a detailed review of the history of Secchi disk). The Secchi disk depth (Z_{SD}, m), a depth when a Secchi disk is no longer viewable by an observer when it is lowered into the water, represents a quantitative measure of the transparency of that water body, or the visibility in the vertical direction (Duntley, 1952). Since the demonstration of transparency measurements with a Secchi disk about 200 years ago (Aas et al., 2014; Wernand, 2010), due to its low cost and easiness to operate, there have been millions of such measurements (along with different sizes of disks) worldwide in the past century (Boyce, Lewis, & Worm, 2012), with Z_{SD} found in a range of a few centimeters for turbid lakes to around 70 m for the clearest oceanic waters (http://www.secchidipin.org/secchi_records.htm). Although more sophisticated optical-electro systems are currently available to measure water quality parameters, Secchi disks are still being widely and regularly used to measure water transparency in both limnology and oceanography studies. Such data are useful to describe the spatial variability of water properties (Arnone, Tucker, & Hilder, 1984; Binding, Jerome, Bukata, & Booty, 2007; Carlson, 1977; Lewis, Kuring, & Yentsch, 1988; Megard & Berman, 1989); to highlight the impact of light availability for the health of substrates (Yentsch et al., 2002); and to show the changes of phytoplankton concentration in the oceans in the past 100 + years (Boyce, Lewis, & Worm, 2010).

The theoretical interpretation of the Secchi disk depth falls into the visual optics of natural waters (Preisendorfer, 1976, 1986) or the underwater visibility theory (Duntley, 1952; Zaneveld & Pegau, 2003) — the branch of the general visibility theory for visual ranging in water. Detailed derivations (also see Section 2) to relate Z_{SD} with water's optical properties can be found in Duntley (1952), Preisendorfer (1976, 1986), Zaneveld and Pegau (2003), and Aas et al. (2014). A general conclusion from these classical works is that Z_{SD} is inversely proportional to the sum of K_d and c within the visible domain, with K_d (m^{-1}) being the

* Corresponding authors.
E-mail addresses: zhongping.lee@umb.edu (Z. Lee), slshang@xmu.edu.cn (S. Shang).

http://dx.doi.org/10.1016/j.rse.2015.08.002

diffuse attenuation coefficient of downwelling plane irradiance and c (m^{-1}) the beam attenuation coefficient. c is an inherent optical property (IOP) (Preisendorfer, 1976) which does not vary with the angular distribution of a light field, while K_d is an apparent optical property (AOP) which does vary with the angular light distribution (Preisendorfer, 1976). Because c is generally 2–5 times or more greater than K_d for wavelengths in the visible domain, in essence Z_{SD} is primarily determined by c following the classical theory. But, numerous measurements (Aas et al., 2014; Bukata, Jerome, & Bruton, 1988; Davies-Colley & Vant, 1988; Effler, 1988; Holmes, 1970; Kratzer, Håkansson, & Sahlin, 2003; Megard & Berman, 1989) have found that: (1) there is no universal relationship between Z_{SD} and c, and: (2) the correlation between Z_{SD} and K_d is typically similar or better than the correlation between Z_{SD} and c. Note that in general K_d and c are two independent optical properties for aquatic environments. In addition, field measurements (Verschuur, 1997) of Z_{SD} show that it varies with sun angle by ~20% between the Sun at zenith and the Sun at 60° from zenith. Such observations are contradictory to the theoretical prediction based on the classical underwater visibility theory. Furthermore, this theory could predict that a half-black–half-white disk will be detectable regardless of its depth in water, which is also contradictory to human experiences (see more detailed discussions in Section 2.2).

These observations and results are quite puzzling, as the underwater visibility theory and the associated models have been the rule in the past 60+ years to theoretically interpret Z_{SD} (Duntley, 1952; Preisendorfer, 1986). Here we revisit the derivations, in particular the key assumptions, associated with the classical visibility theory (CVT) and discuss the likely lapses in that theory for the inconsistency between the theoretical predictions and observations. We further propose a new theory and a mechanistic model to interpret and estimate Z_{SD}, which we subsequently verify with independent measurements from a wide range of aquatic environments.

2. The century-old theory for underwater visibility

2.1. Theoretical derivations

Consider a Lambertian disk placed horizontally at a depth z in water which is viewed by a snorkeler just below the surface (see Fig. 1). Following radiative transfer theory, the radiance over the target (L_T) propagating upward towards the snorkeler can be expressed as (Aas et al., 2014; Duntley, 1952; Højerslev, 1986; Preisendorfer, 1986; Zaneveld & Pegau, 2003),

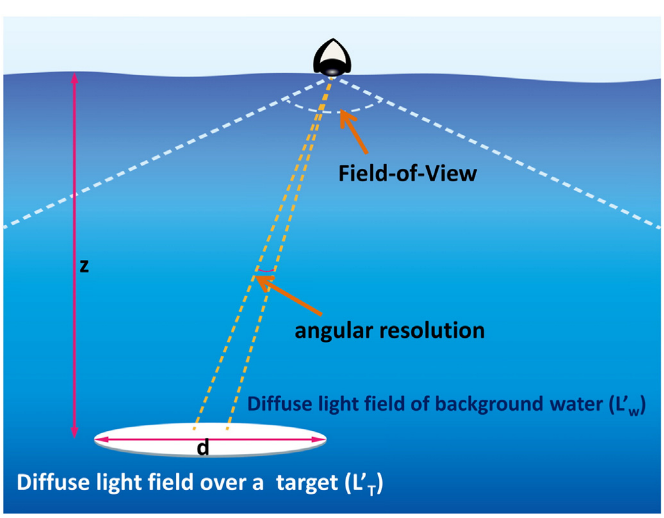

Fig. 1. A cartoon showing how the light over an underwater target and that of the background are detected by a surface snorkeler.

$$\frac{d\,L_T(z)}{dz} = -c\,L_T(z) + \int_{4\pi} L'_T(z,\theta,\varphi)\beta(\theta,\varphi)d\omega, \quad (1)$$

with L'_T the radiance distribution in the 4π direction above the target and β the volume scattering function of water (see Table 1 for notations; here the wavelength dependence is omitted for brevity). Note that here we use radiometric rather than photometric quantities (Aas et al., 2014; Duntley, 1952; Højerslev, 1986; Preisendorfer, 1986; Zaneveld & Pegau, 2003) to discuss the concepts and assumptions taken by the CVT in interpreting Secchi disk depth, as the concepts and assumptions remain the same in both radiometric and photometric formulation.

Similarly the upward radiance of the adjacent water without the disk (L_w) is given by

$$\frac{d\,L_w(z)}{dz} = -c\,L_w(z) + \int_{4\pi} L'_w(z,\theta,\varphi)\beta(\theta,\varphi)d\omega, \quad (2)$$

with L'_w the radiance distribution of the background (reference) in the 4π direction. In all historical derivations (Aas et al., 2014; Duntley, 1952; Preisendorfer, 1986; Zaneveld & Pegau, 2003), it was assumed that

$$\int_{4\pi} L'_T(z,\theta,\varphi)\beta(\theta,\varphi)d\omega = \int_{4\pi} L'_w(z,\theta,\varphi)\beta(\theta,\varphi)d\omega, \quad (3)$$

Table 1
Notations.

Symbol	Description	Unit
β	Volume scattering function of water	$\mathrm{m}^{-1}\ \mathrm{sr}^{-1}$
b_f	Forward scattering coefficient	m^{-1}
c	Beam attenuation coefficient	m^{-1}
C_a	Apparent contrast	–
C_a^n	New apparent contrast	sr^{-1}
C_i	Inherent contrast	–
C_i^n	New inherent contrast	sr^{-1}
C_t	Contrast threshold of human eye	–
C_t^r	Contrast threshold of human eye in radiance reflectance	sr^{-1}
[Chl]	Concentration of chlorophyll	$\mathrm{mg/m^3}$
E_d	Downwelling irradiance	$\mathrm{W/m^2/nm}$
K_d	Diffuse attenuation coefficient of downwelling plane irradiance	m^{-1}
K_d^{pc}	Depth-averaged diffuse attenuation coefficient of downwelling irradiance at the wavelength of perceived color	m^{-1}
K_d^{tr}	Depth-averaged diffuse attenuation coefficient of downwelling irradiance in the spectral transparent window	m^{-1}
K_T^{tr}	Depth-averaged diffuse attenuation coefficient of radiance reflected by a target and in the spectral transparent window	m^{-1}
L_w	Upwelling radiance of adjacent water without a disk	$\mathrm{W/m^2/nm/sr}$
L'_T	Radiance distribution over the target	$\mathrm{W/m^2/nm/sr}$
L'_w	Radiance distribution over the background	$\mathrm{W/m^2/nm/sr}$
L_T	Upwelling radiance over the area with a target	$\mathrm{W/m^2/nm/sr}$
$L_T^{tr}(0-)$	Upwelling radiance just below the surface of the target area	$\mathrm{W/m^2/nm/sr}$
$L_w^{tr}(0-)$	Upwelling radiance just below the surface of the background area	$\mathrm{W/m^2/nm/sr}$
L_C^{tr}	Contrast in radiance between the disk and no-disk areas	$\mathrm{W/m^2/nm/sr}$
r_T	Radiance reflectance right above a target	sr^{-1}
r_w	Radiance reflectance of background (water)	sr^{-1}
V_w	Visibility in horizontal direction	m
z	Water depth	m
Z_{SD}	Secchi disk depth or vertical visibility	m

and subtraction of Eqs. (1) and (2) resulted in

$$\frac{d\,(L_T(z) - L_w(z))}{dz} = -c(L_T(z) - L_w(z)). \quad (4)$$

Assuming the water is homogeneous, integrating Eq. (4) from depth to surface results in

$$(L_T(0) - L_w(0)) = (L_T(z) - L_w(z))\, e^{-cz}. \quad (5)$$

Further, in the CVT, the apparent contrast (C_a) between the target and the background (or reference) is defined as

$$C_a = \frac{L_T(0) - L_w(0)}{L_w(0)}. \quad (6)$$

The solar irradiance propagating from surface to depth generally follows an exponential decline function (Gordon & Morel, 1983)

$$E_d(z) = E_d(0-)\, e^{-K_d z}. \quad (7)$$

Applying Eqs. (6) and (7) to Eq. (5) leads to

$$C_a = C_i e^{-(K_d + c)z}, \quad (8)$$

with the inherent contrast, C_i, defined as (Aas et al., 2014; Duntley, 1952; Preisendorfer, 1986; Zaneveld & Pegau, 2003)

$$C_i = \frac{r_T - r_w}{r_w}. \quad (9)$$

Here r_T and r_w are the reflectance of the target (measured right above it) and the background, respectively. Eq. (8) forms the Law of Contrast Reduction (Duntley, 1952; Preisendorfer, 1986), which is the core of the classical theory for visibility in both air and water, and has been adopted by the research community for more than 60 years to interpret underwater visibility. Such a Law of Contrast Reduction is the same as that used for visual ranging in air (Middleton, 1952).

When C_a matches the threshold of eye detection (C_t), the visibility in the vertical direction (Z_{SD}, or V_{-90} in Duntley (1952)), is given by

$$Z_{SD} = \frac{1}{K_d + c} \ln\left(\frac{1}{C_t} \frac{r_T - r_w}{r_w}\right). \quad (10)$$

Further, if the target is black ($r_T = 0$, i.e., negative contrast between the target and the background) and viewed horizontally, the maximum horizontal detectable distance is (Duntley, 1952; Preisendorfer, 1986; Zaneveld & Pegau, 2003)

$$V_w = \frac{-\ln(C_t)}{c}. \quad (11)$$

As Duntley (1952) pointed out, Eq. (11) is in an identical form as the Koschmieder theory established 90 years ago for visibility in the air (Middleton, 1952). Furthermore, because c is an IOP, the predicted horizontal visibility is independent of the azimuth viewing direction (or the background) for a given threshold, which thus actually represents an easy-to-understand index for the quality of atmosphere or water.

Eqs. (10) and (11) become the key analytical models for visibility applications in air and water in the past 60+ years. And, for the above derivations, Eq. (3) is the critical assumption. The validity of this assumption, however, as discussed in detail below, may not be assumed automatically for visual ranging.

2.2. Caveats in the classical theory and associated model

2.2.1. The attenuation of contrast

The beam attenuation coefficient (c) is used in the CVT to propagate the contrast of a finite-size target (Eqs. (5) and (8)), where by definition c represents the attenuation of a collimated light beam (Preisendorfer, 1976). In the theoretical derivations to reach Eqs. (5) and (8), there was no consideration of the unique high-angular resolution of human eyes; and the relative size between the target and the viewing distance (see Fig. 1) is ignored. Basically, the target is treated as a small object, leading to the assumption that both sides of Eq. (3) can be assumed to equal each other. This assumption is the key for the resulted contrast propagation (Eq. (5)) and the Law of Contrast Reduction for a vertically-viewed target (Eq. (8)). This assumption is generally appropriate for the visibility theory in air where the maximum viewable distance is often in the order of several tens of kilometers and the target (a finite size black object) is in the order of meters (Middleton, 1952). For a target in water (such as a Secchi disk or a diver, which is usually several tens of centimeters or larger), because of the significantly higher absorption and scattering coefficients of water constituents than that of air molecules (Kirk, 1994; Middleton, 1952), the maximum viewable distance is at most several tens of meters, i.e., ~1/1000 of that in air, consequently the validity of Eq. (3) is in question.

The "measurement" or detection of a target by the human eye is very different from that by an eletro-optic sensor (Duntley, 1952), where the eye–brain system is an optical imager with an array of millions of "tiny-sensors". For a healthy eye system, it can collect information simultaneously for targets in a range of ~160° × 175° (although the actual imaging region is smaller than this). Such a unique combination enables simultaneous observations of the target and the background (or reference), which is the key for target sighting under varying environmental lighting. The angular resolution of the human eye is ~0.5 arcmin (equivalent to a spatial resolution of ~0.2 mm from a distance of 1 m) (Clark, 1990; Curcio, Sloan, Kalina, & Hendrickson, 1990). This is equivalent to a digital camera with ~600 Megapixels, thus enables the collection of radiance at very fine resolutions, which is why we can see fine details of a target and how we can read.

Due to this extremely fine resolution of the human eye, the relationship between the pixel size of the collected image and the size of a target will depend on the distance (z) and the size of the target (d, see Fig. 1). In the water Z_{SD} is often several tens of meters, resulting in a pixel size of several millimeters. Thus, a Secchi disk is much larger than the pixel size and can no longer be considered as a point source. Consequently, the radiance distribution over a Secchi disk could be very different from that over the nearby background. This unique feature and phenomenon are demonstrated in Fig. 2 for a black-and-white disk in water pictured with a digital camera ~1 m above the disk. For a point (B) over the disk and a point (A) in the adjacent water (both at same depth), their surrounding light (represented by the brown dashed line above each letter in the right side of Fig. 2) are $L'_T(z, B)$ and $L'_w(z, A)$, respectively. Because the radiance distribution is generally not uniform at a given depth (especially for depths closer to the target) due to the intrusion of this target, there is in general:

$$L'_T(B, z) \neq L'_w(A, z). \quad (12)$$

Therefore Eq. (3) is not always true for a Secchi disk or large objects, especially for depths closer to the target (Aas et al., 2014). One exception is when points A and B are two adjacent pixels (such as a point-source target, or when B is at the edge of a finite-size target while A is an adjacent water pixel), the two brown dashed lines will approach each other and the approximation of Eq. (3) could then be valid. The sighting of a Secchi disk in water, however, is generally not determined based on the contrast between its edge and the adjacent water, but rather based on the detection of any portion of the disk that has the highest contrast from the background. In general the distance between points A

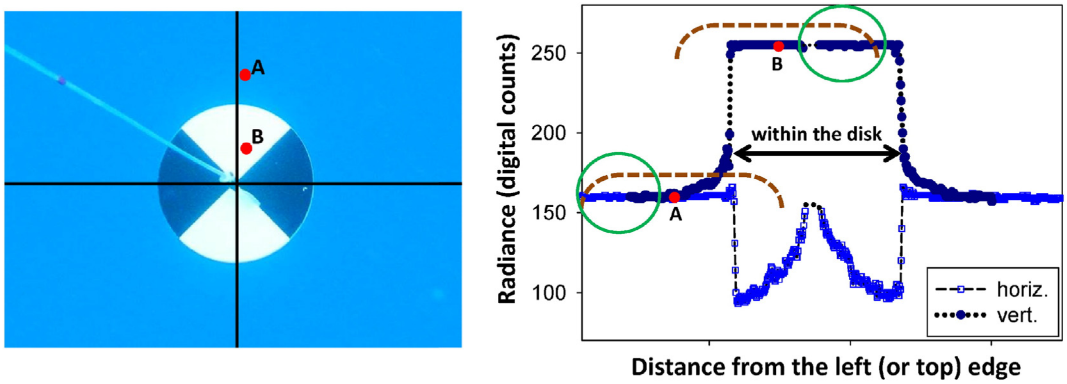

Fig. 2. (left) An alternating-black-and-white Secchi disk in blue water observed vertically. (right) Variation of radiance (digital counts) for pixels on the black lines of the Secchi disk image. Points A and B indicate likely locations for judgment decisions on whether the disk is still discernable by a human eye, with the brown dashed lines indicating the range of radiance that could be used in Eq. (3) for integrations. Radiance within the green circles indicates those outside of the overlap that are used in Eq. (3). Note that the digital camera was saturated for radiance over the white portion of the disk, while the radiance over the black portion of the disk increases towards the center due to adjacent contributions from the white portion of the disk. Radiance at the center of the disk is omitted due to interference of the holding string.

and B is likely 10's to 100's of pixels. In these cases, after subtracting the overlapping potions of $L'_T(z, B)$ and $L'_w(z, A)$, an exact Eq. (4) in the above derivations for points A and B would be:

$$\frac{d\,(L_T(z,B)-L_w(z,A))}{dz} = -\,c(L_T(z,B)-L_w(z,A)) + \left(\int_{[\zeta]} L'_T(z,B,\zeta)\beta(\zeta)d\omega - \int_{[\xi]} L'_w(z,A,\xi)\beta(\xi)d\omega\right), \tag{13}$$

with [ζ] and [ξ] representing the residual solid angles outside of the overlapping range between points A and B, shown as the circled portions in the right side of Fig. 2. We may further divide the radiances within [ζ] and [ξ] as the upward and downward radiances following Zaneveld (1995). Because downward radiance is mainly determined by incident light, $L'_T(z,B,\zeta_d)$ is approximately $L'_w(z,A,\xi_d)$. For upward radiance, $L'_T(z,B,\zeta_u)$ and $L'_w(z,A,\xi_u)$ contribute to $L_T(z,B)$ and $L_w(z,A)$, respectively, through forward scattering (Zaneveld, 1995). Therefore, Eq. (13) can be written as

$$\frac{d\,(L_T(z,B)-L_w(z,A))}{dz} = -\,c(L_T(z,B)-L_w(z,A)) + \,\varepsilon b_f(L_T(z,B)-L_w(z,A)), \tag{14}$$

which further leads to a more generalized equation for contrast propagation

$$(L_T(0)-L_w(0)) = (L_T(z)-L_w(z))\,e^{-(c-\varepsilon b_f)z}. \tag{15}$$

The value of parameter ε depends on the distance (i.e. size of the target) between points A and B. For a small target, ε approaches 0, and contrast propagation follows the beam attenuation coefficient; for a large target, because of contributions from forward scattering of adjacent pixels within the target, ε is greater than 0 and the attenuation of contrast no longer follows the beam attenuation coefficient. This dependence of attenuation on target sizes is consistent with conclusions regarding image propagation through a media (Hou, Lee, & Weidemann, 2007; Wells, 1973a, b), where the attenuation of high-spatial-frequency images (small objects or narrow beam) follows c (which is the sum of absorption and scattering coefficients) while the attenuation of low-spatial-frequency images (large objects or broad beam) follows the sum of absorption coefficient and a portion of the scattering coefficient (Wells, 1973a, b). In short, for visual ranging of a target in water or air, if the size of the target is much larger than the spatial resolution of a human eye, Eq. (3) is not necessarily valid, the Law of Contrast Reduction (Eq. (8)) could not be derived, and then visibility models (Eqs. (10) and (11)) based on this theory may not be appropriate. Such a caveat associated with the CVT can also be explained as follows. If Eq. (5) is valid, mathematically it will lead to,

$$(L_T(0)-L_T(z)\,e^{-cz}) = (L_w(0)-L_w(z)\,e^{-cz}). \tag{16}$$

For this to be satisfied for any c and z, the following relationships must be true,

$$L_T(0) = L_T(z)\,e^{-cz} + X(z), \tag{17a}$$

$$L_w(0) = L_w(z)\,e^{-cz} + X(z). \tag{17b}$$

Here $X(z)$ is a function of z (such as the path radiance between depth z and surface) and becomes 0 when z is 0. Radiative transfer theory tells us that Eq. (17a) is valid only for a point source or small target.

This caveat associated with the contrast attenuation of a Secchi disk in the CVT could be the fundamental reason why many studies have shown that the estimated Z_{SD} based on the classical theory agree poorly with observations (Bowers et al., 2000; Doron, Babin, Hembise, Mangin, & Garnesson, 2011; Morel et al., 2007; Zhang, Wei, Lin, & Shang, 2014). Instead of questioning the assumptions behind the theory, the discrepancies between the modeled and observed Z_{SD} were often implicitly attributed to measurement errors or algorithms to estimate the IOPs.

In addition, there have been numerous reports showing c-based empirical models of Z_{SD} (Aas et al., 2014; Bukata et al., 1988; Davies-Colley & Vant, 1988; Devlin et al., 2008; Gallegos, Werdell, & McClain, 2011; Holmes, 1970; Megard & Berman, 1989). Although strong correlations (R^2 ~ 0.9 in general) were presented for each dataset, the slopes between the modeled and measured Z_{SD} show a rather wide range of variations even for measurements of nearby lakes obtained by the same researchers (e.g., Bukata et al. (1988)). Sometimes for data from the same group, the measurements of $Z_{SD} < 2$ m have to be excluded in order to obtain a good fit with the c-based formula (Aas et al., 2014). These results indicate further that there does not exist a single and globally applicable relationship between Z_{SD} and c (or $c + K_d$ as c is ~2–5 times or more larger than K_d) for global waters (Gordon, 1978). This non-uniformity, again, could be mainly due to the assumption of Eq. (3).

The sighting of a black disk horizontally just below the surface may be a special case (Davies-Colley & Vant, 1988; Zaneveld & Pegau, 2003). In this scenario, while the distance between points A and B could still be relatively wide (compared to eye resolution), the approximation of Eq. (3) might still be valid. This may occur because most of the surrounding light over the target and the background are strong radiances in the horizontal directions as demonstrated with field observations (Zaneveld and Pegau, 2003).

2.2.2. Contrast for visual judgment (C_i and C_a)

In the CVT, the contrast for visual judgment (C_i and C_a) is defined as a relative difference of radiance (or reflectance) between the target and the background or reference (Eq. (6) or Eq. (9)) (Aas et al., 2014; Duntley, 1952; Preisendorfer, 1986; Zaneveld & Pegau, 2003). This definition and application of contrast provide a good measure of the sharpness of a picture, but is subjective to the use of "background" or "reference" and may result in false prediction of target sighting as the maximum C_i value is infinite. For instance, for an alternating-black-and-white disk (usually used in limnology studies), the C_i value approaches infinite when the black side is considered as the background or reference. With this formulation for contrast the Secchi disk should be detectable even at hundreds of meters deep as the calculated apparent contrast (Eq. (8)) would still be greater than the eye threshold. Or, for a white cup filled with black coffee, the white bottom of the cup should be always viewable regardless of the cup's depth as C_i approaches infinite when the black coffee is considered as the background.

Such contradictions can be further demonstrated with a hypothetical scenario. Assuming a 90-m deep bottom under clear waters (e.g., those in the Caribbean) and the bottom is sharply divided into two sides with different bottom types, one side is black bottom (near 0 reflectivity) and the other side (the target) is quartz sand bottom (50% reflectivity). The water has a chlorophyll concentration ([Chl]) of 0.1 mg/m^3 and all optical properties following the Case-1 scheme (Morel & Maritorena, 2001). Fig. 3 shows the subsurface radiance reflectance (r, sr^{-1}) of the two sides simulated by Hydrolight (Mobley & Sundman, 2013), along with C_a calculated between the two sides following Eq. (6). Value of C_a (see Fig. 3) in the spectral window around 490 nm is ~0.9% (contrast becomes ~0.2% when using spectrally-integrated luminance), which jumps to ~5.5% if the bottom is uplifted to 70 m (contrast becomes ~1.4% when using spectrally-integrated luminance). These values are around or higher than the 0.66% threshold for detection by the human eye as suggested for Secchi disk sighting (Højerslev, 1986; Preisendorfer, 1986; Tyler, 1968). However, such visual sightings have never been reported in the literature or news. In contrast, reports for sighting bright bottoms in clear waters are in the range of 20–30 m. In addition, these C_a values are much smaller than that would be predicted by Eq. (8) as the inherent contrast between the two sides approach infinite with the black side as the background.

Fundamentally, target sighting by the eye-brain system depends on where there is sufficient difference in the radiance (or brightness) between the target and the background (reference) when there is no difference in color (Blackwell, 1946). This difference in radiance changes with both the incident light and the difference in reflectivity between the target and the background. On the other hand, the sensitivity of the human eye also adapts to the intensity of the ambient light. Therefore, what really matters for this judgment decision under the photopic vision regime (i.e., light intensity is in a range of usual indoor to outdoor light) is the difference in reflectivity between the target and the background, or the so called "brightness constancy" concept of visual perception (Bartleson & Breneman, 1967; Freeman, 1967). Specifically, it means "… judgments of brightness have been shown to be dependent not on the quantity of light entering the eye, but rather on the reflectance of the surface from which luminous energy is reflected" (Freeman, 1967). This is why we perceive a black–white checker board nearly the same under either sunshine or tree shadows. The definition and application of relative difference in radiance or reflectance as the contrast in the CVT, however, is not consistent with the "brightness constancy" concept in visual perception. It is following this brightness constancy concept that a new theory for underwater visibility is formulated.

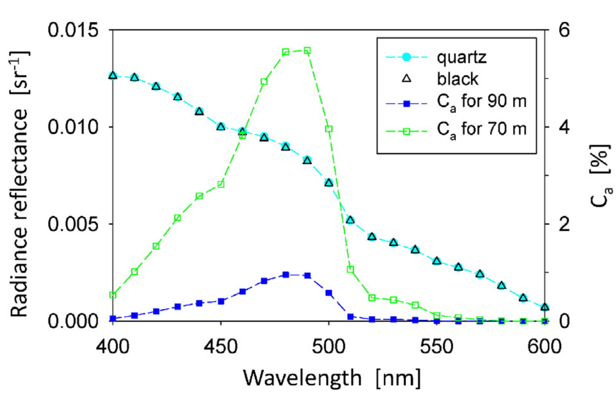

Fig. 3. An example showing how the contrast evaluation in classical underwater visibility theory would result in likely false prediction of detecting a half-bright–half-black bottom in deep clear waters. The y-axis to the left shows the radiance reflectance of clear waters just below the surface ($r(0-)$, sr^{-1}) with a highly reflecting quartz (solid circle) and black (open circle) bottom at 90 m depth. The y-axis to the right shows the apparent contrast (Eq. (6), square symbol). Open square represents the apparent contrast if the quartz/black bottom is uplifted to 70 m.

3. New theory for underwater visibility

The ultimate goal of a generalized visibility theory is to express parameter ε in Eq. (15) as a function of both target size and distance for any light illumination conditions. This will require not only complex derivations based on radiative transfer, but also sophisticated and carefully designed field experiments for different objects under various conditions. Here the problem is simplified to Secchi disks only and viewed vertically by a human eye in the photopic vision regime. As discussed in details in Section 2, a regular Secchi disk (~30 cm in diameter) in the viewable range in water is significantly larger than the size of an image pixel of a human eye (generally $d/Z >>$ angular resolution and within the FOV of a human eye), thus we may consider this target as a large bottom for the array of tiny sensors of a human eye when observed vertically at surface (see Fig. 1). The upwelling radiance just below the surface from pixels within such a target can then be considered to follow the relationships established for optically shallow waters (Albert & Mobley, 2003; Lee, Carder, Mobley, Steward, & Patch, 1998; Lyzenga, 1981; Philpot, 1989; Voss, Mobley, Sundman, Ivey, & Mazel, 2003)

$$L_T(0-) = r_w E_d(0-)\left(1-e^{-(K_d+K_T)\,z}\right) + r_T E_d(0-) e^{-(K_d+K_T)\,z}. \tag{18}$$

Here $L_T(0-)$ represents the radiance signal (after integration from the target depth to surface) reaching the eye system, with $E_d(0-)$ the incident downwelling irradiance just below the surface. r_T and r_w are the radiance reflectance of a Secchi disk and background water, respectively. K_d (m^{-1}) is the depth-averaged diffuse attenuation coefficient of plane downwelling irradiance, while K_T (m^{-1}) is the depth-averaged diffuse attenuation coefficient of the upwelling radiance arising from the target reflection. Here wavelength dependence is omitted for brevity unless it is necessary.

For adjacent water pixels (outside the glow of the disk where the adjacency effect is minimal) that serve as the background, the total upwelling signal just below the surface is

$$L_w(0-) = r_w E_d(0-). \tag{19}$$

Because visual perception of a target by the human eye is based on the detection of enough difference in brightness (radiance) and/or color between the target and the reference (Blackwell, 1946), the contrast in radiance reaching a human eye is calculated as

$$L_C(0-) = |L_T(0-) - L_w(0-)|. \tag{20}$$

Applying Eqs. (18) and (19), Eq. (20) becomes

$$L_C(0-) = |r_T - r_w| E_d(0-) e^{-(K_d+K_T)\,z}. \tag{21}$$

This expression is conceptually consistent with Eq. (15) for contrast attenuation as generally the diffuse attenuation coefficient is a function of total absorption and backscattering coefficients (Gordon, 1989; Lee, Du, & Arnone, 2005). Similarly ($c - \varepsilon\, b_f$) of Eq. (15) also represents a function of total absorption and backscattering coefficients as ε approaches 1 for large targets (Wells, 1973a, b).

3.1. Secchi disk detection by a human eye: spectral information of a target

Detection of a target by the eye–brain system uses both intensity and color contrast. In particular, a human eye can distinguish millions of colors in the visible domain (Judd & Wyszecki, 1975), which translates to thousands of spectral bands in the 400–700 nm range with each band at 1-nm bandwidth. For sighting a target in air, while the relative contribution of light from the target will decrease at each wavelength with the increase of distance, this reduction is nearly the same across the visible domain, i.e. there will be little change in the apparent color of the target at distance. In short, the transmittance in air is spectrally neutral (except for the narrow absorption bands of atmosphere gases or smokes) in general, and this spectral neutrality remains nearly the same for different visibility ranges. Consequently photometric (brightness) quantities are used for the evaluation of contrast for a white or black target in air, and this approach was adopted in the classical underwater visibility theory (Preisendorfer, 1986; Zaneveld & Pegau, 2003).

Because of the spectrally selective nature of the absorption and scattering properties of water constituents (Kirk, 1994; Mobley, 1994), however, spectral quality is no longer the same for observing a target in water. When a Secchi disk is lowered in water and observed by a human eye at the surface, the relative contribution of light from the Secchi disk will decrease with the increase of depth. This reduction, however, is strongly spectrally dependent and photons reflected by the Secchi disk that reach a human eye very quickly narrow to waters' spectrally transparent window. In short, when a Secchi disk is lowered deeper and deeper, there are changes in both brightness and color between the area containing the Secchi disk and the adjacent water, and eventually the difference in color diminishes (Aas et al., 2014) and the contrast in brightness at this color (wavelength) becomes below the detection threshold of a human eye. This phenomenon is illustrated in Fig. 4, where Fig. 4a shows the change of spectral radiance with increasing Secchi disk depth (simulated with Eq. (18)), while Fig. 4b shows the corresponding colors in CIE chromaticity diagram (Mobley, 1994) perceived by a human eye and the dominant wavelengths. For clear water ([Chl] = 0.1 mg/m^3) with the disk 5 m below the surface, there is not only a strong difference in radiance (brightness) between the target and the background, but also a rather big difference in color, with the target and the background centered at 486 nm and 478 nm, respectively. When the disk gets to 40 m below the surface (a depth approaching the limitation of detection), the difference in radiance (brightness) between the target and the background is significantly reduced, and the color of the target (479 nm) approaches that of the background (478 nm). It is therefore reasonable to hypothesize that the detection of a Secchi disk in water by a human eye depends on the contrast of brightness in the spectral window of the perceived water color; whereas this spectral window changes significantly from water to water. Experimental proof of this hypothesis is beyond the scope of the current work as it would require sophisticated equipment and field-based measurements in different water environments. However, such a hypothesis is supported by the results shown later.

The contrast of brightness at the wavelength corresponding to the color perceived by a human eye when the Secchi disk starts to disappear can be written as

$$N_C^{pc}(0-) = \left|r_T - r_w^{pc}\right| H_d^{pc}(0-)\, e^{-\left(K_d^{pc}+K_T^{pc}\right)\,z}. \tag{22}$$

Here N_C represents the contrast in luminance recorded by a human eye, H_d is the equivalent input illuminance, and the superscript "pc" stands for the perceived color by a human eye and each color is associated with a specific wavelength (see Fig. 4). K_d^{pc} and K_T^{pc} in Eq. (22) are the depth-averaged diffuse attenuation coefficients of the downwelling plane irradiance and upwelling radiance arising from the target reflection at the wavelength of the perceived color, respectively.

Because there have been no measurements or studies of K_d specifically for the human eye perceived color, we rely on the modeling of K_d^{pc} for waters with a wide range of chlorophyll concentrations (see Appendix A for details of this modeling). It is found that K_d^{pc} can be well represented by the minimum K_d within the visible domain (400–700 nm) (see Fig. 5), which is the attenuation coefficient of the transparent window of the water column (K_d^{tr}). We use this diffuse attenuation coefficient to approximate K_d^{pc} and K_T^{pc}, respectively, in the following for easy computation, and rewrite Eq. (22) as,

$$N_C^{pc}(0-) = \left|r_T - r_w^{pc}\right| H_d^{pc}(0-) e^{-\left(K_d^{tr}+K_T^{tr}\right) z}, \tag{23}$$

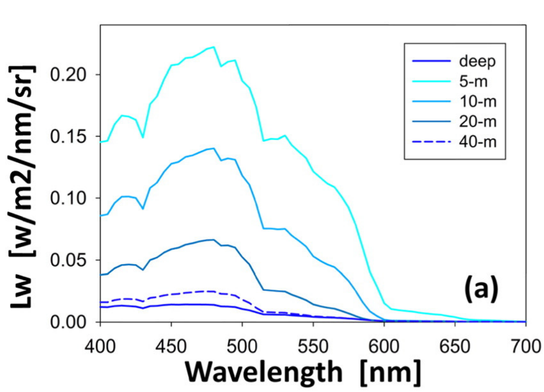

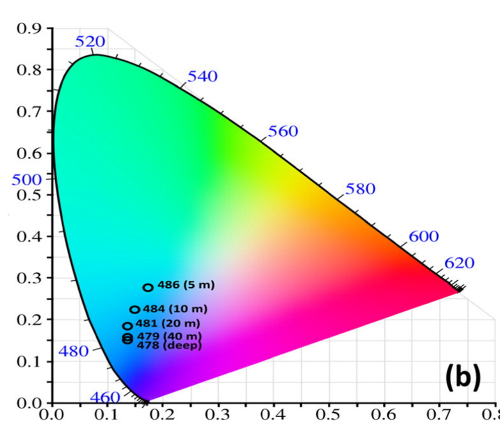

Fig. 4. Illustration of changes of brightness (radiance) and color when a Secchi disk is lowered in deep blue water, where the color difference between the two disappears when the disk is approaching 40 m. (a) Spectral radiance (Lw) of the water without the Secchi disk ("deep" in the legend, [Chl] = 0.1 mg/m^3) and spectral radiance of the water area containing a Secchi disk (with a reflectance as 0.85) at different depths (modeled with Eq. (18)). All are under a clear sky with the Sun at 30° from zenith. (b) The perceived colors by the human eyes and their dominant wavelengths (annotated with circles) for the corresponding radiance spectra on the left. Here the x- and y-axes represent the two normalized values of the three tristimulus values. Note that when the disk is 40-m deep the wavelength (479 nm) corresponding to the human perceived color is very close to the wavelength (478 nm) from the nearby waters (the background). The background CIE chromaticity diagram is a courtesy of Wikipedia.

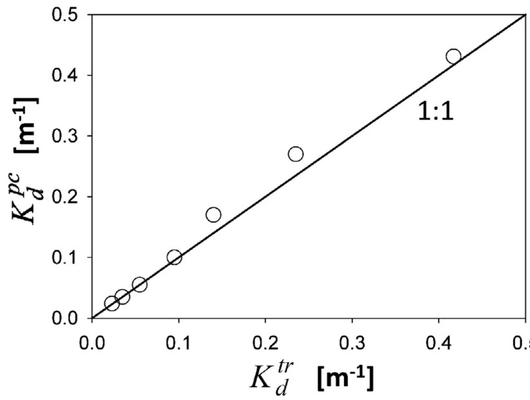

Fig. 5. Relationship between diffuse attenuation coefficient at the wavelength of the perceived color (K_d^{pc}) and diffuse attenuation coefficient of the transparent window (K_d^{tr}) for waters with [Chl] as 0.03, 0.1, 0.3, 1, 3, 10, and 30 mg/m^3. Details of the simulations are provided in Appendix A. These results suggest that K_d^{pc} can be approximated by K_d^{tr} for the interpretation of Secchi disk depth.

with K_d^{tr} and K_T^{tr} the depth-averaged diffuse attenuation coefficient of the downwelling irradiance and upwelling radiance arising from the target reflection at the transparent window of the water, respectively.

3.2. Secchi disk detection by a human eye: contrast for judgment decision

Detection of a target by a human eye requires that N_C is greater than a threshold. On the other hand, this threshold also varies with the intensity of ambient light (Blackwell, 1946), thus a more applicable evaluation of the contrast for the target detection is the ratio of N_C to H_d. This is consistent with the "brightness constancy" concept for visual perception under the photopic vision regime (Bartleson & Breneman, 1967; Freeman, 1967). Therefore a new apparent contrast (C_a^n, sr^{-1}) is defined as

$$C_a^n = \frac{N_C^{pc}(0-)}{H_d^{pc}(0-)}. \tag{24}$$

Applying Eq. (23) we obtain

$$C_a^n(0-) = |r_T - r_W^{pc}| e^{-(K_d^{tr}+K_T^{tr})z}. \tag{25}$$

This further leads to a new Law of Contrast Reduction for sighting a Secchi disk as

$$C_a^n = C_i^n e^{-(K_d^{tr}+K_T^{tr})z}, \tag{26}$$

with C_i^n the new inherent contrast and defined as

$$C_i^n = |r_T - r_W^{pc}|. \tag{27}$$

Compared to the contrast evaluation in the CVT (Eq. (9)), now the contrast is evaluated as the absolute difference in reflectance between the target and the background (or reference). With such a formulation, the maximum value of C_i^n is limited by the reflectance of the target or the background. For an alternating-white–black disk as that usually used in limnology studies, the inherent contrast will then become r_T of the white side when the black side is considered as the reference (assuming black side has a reflectance as 0). This value is just slightly larger than the contrast between the white disk and the water, which then explains why the observed Z_{SD} were nearly the same between using completely white disks and using alternating-white–black disks. In the following, since reflectance in a narrow spectral band is the same for both radiometric and photometric quantities, radiometric quantities are employed for the derivation and discussion of Secchi disk depth.

3.3. New mechanistic model for Secchi disk depth

When C_a^n matches the contrast threshold ($C_t^r(0-)$, sr^{-1}, i.e. measured in sub-surface radiance reflectance) for target detection by the eye-imager, the maximum detectable distance of this disk in the vertical direction or vertical visibility (Duntley, 1952) becomes

$$Z_{SD} = \frac{1}{K_d^{tr} + K_T^{tr}} \ln\left(\frac{|r_T - r_W^{pc}|}{C_t^r(0-)}\right). \tag{28}$$

The diffuse attenuation coefficient (K_d) is generally a function of IOPs and solar elevation (Gordon, 1989; Lee et al., 2005). For easier data processing, considering $K_T^{tr} \approx 1.5\,K_d^{tr}$ for the upwelling radiance arising from the reflection by a Lambertian bottom and for the Sun high above the horizon (Kirk, 1991; Lee et al., 1994; Lee et al., 1998), Secchi disk depth described by Eq. (28) can be approximated as

$$Z_{SD} = \frac{1}{2.5K_d^{tr}} \ln\left(\frac{|r_T - r_W^{pc}|}{C_t^r(0-)}\right). \tag{29}$$

Eqs. (26)–(28) form the core of the new underwater visibility theory and mechanistic models to interpret Secchi disk depth. Compared to the CVT, the new visibility theory provides a mechanistic explanation for the numerous observations over the past many decades that there is a strong inverse relationship between Z_{SD} and the diffuse attenuation coefficient (Holmes, 1970; Kratzer et al., 2003; Megard & Berman, 1989; Padial & M. Thomaz, 2008). Also, with the new visibility theory and model the bottom of a regular-size white cup filled with black coffee or a 70-m deep half-bright–half-black bottom in clear waters will not be detectable under the photopic vision regime (because the inherent contrast is now limited), which is consistent with our observations.

4. Verification of the new model with independent measurements

The establishment of the new visibility theory and its associate model (Eqs. (28)–(29)) is based entirely on radiative transfer theory. In addition to the above theoretical arguments, their ultimate verification requires concurrent measurements of visibilities and water optical properties (spectral r_w, K_d and K_T) over a wide dynamic range of environments. This is a prerequisite rarely met. However, by searching the SeaWiFS Bio-optical Archive and Storage System (SeaBASS) database, a dataset with 144 measurements containing both Z_{SD} and $R_{rs}(\lambda)$ was found for waters around the USA, with R_{rs} (sr^{-1}) being the above-surface remote-sensing reflectance (Mobley, 1999). In addition, a total of 197 data points having both Z_{SD} and R_{rs} were compiled from measurements of oceanic and coastal waters off China (Shang et al., 2011). This combined dataset covers oceanic, coastal, and lake waters (see Fig. 6a for locations), where Z_{SD} ranges between 0.1 and 30 m and R_{rs} values are provided at 412, 443, 488, 532, 555 and 665 nm, with measurements conducted independently by many research groups.

Because Secchi disk depth was determined from viewers above the surface, the radiance contrast in air (L_C^{tr}) must be used, which is written as

$$L_C^{tr}(0+) = \left|\left(\frac{t}{n^2}L_T^{tr}(0-) + L_{T-sky}^{tr}\right) - \left(\frac{t}{n^2}L_W^{tr}(0-) + L_{W-sky}^{tr}\right)\right|. \tag{30}$$

Here t is the radiance transmittance across the water-air interface and n is the refractive index of seawater; while L_{T-sky}^{tr} and L_{W-sky}^{tr} are the surface-reflected skylight of the target and the reference areas in the transparent window of water, respectively. Assume L_{T-sky}^{tr} and L_{W-sky}^{tr} are the same during the observations, after converting the

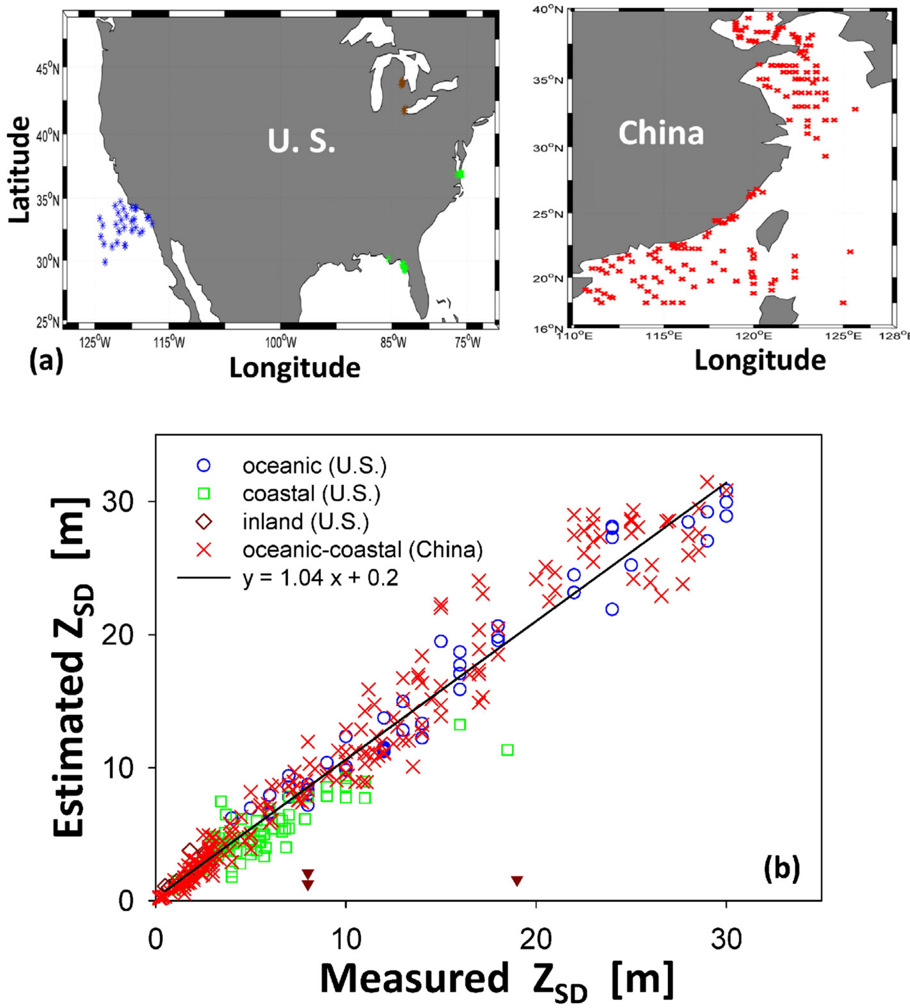

Fig. 6. (a) Locations of field measurements, with data obtained from NASA's SeaBASS archive and measured in oceanic and coastal waters off China. (b) Comparison between measured and predicted vertical visibility with the mechanistic model (and its coefficients) developed following the new underwater visibility theory. The three red points were considered as outliers (the measured reflectance of these points are extremely different from those of waters with identical or similar Z_{SD} values) and were excluded in the model verification. If included, the mean absolute percent difference increases from 18.2% to 19.3%.

radiance contrast to reflectance contrast (i.e., divided by $E_d^{tr}(0+)$, and note that $E_d^{tr}(0-) = t\,E_d^{tr}(0+)$), there is

$$C_a^n(0+) = \frac{t^2}{n^2}\left|r_T - r_w^{pc}\right| e^{-\left(K_d^{tr}+K_T^{tr}\right)z}. \tag{31}$$

Lastly the visibility equivalent to Eq. (29) for an above-surface observer is

$$Z_{SD} = \frac{1}{2.5K_d^{tr}}\ln\left(\frac{t^2}{n^2}\frac{\left|r_T - r_w^{pc}\right|}{C_t^r}\right), \tag{32}$$

with C_t^r (sr^{-1}) the detection threshold of the human eye in air.

To obtain the required K_d information for the estimation of Z_{SD}, the R_{rs} values were first fed to the latest version (http://www.ioccg.org/groups/software.html) of the Quasi-Analytical Algorithm (Lee, Carder, & Arnone, 2002) to obtain total absorption (a) and backscattering (b_b) coefficients. Subsequently K_d at 443, 488, 532, 555 and 665 nm were derived from a and b_b following the IOP-based model (Lee et al., 2005; Lee et al., 2013) by assuming a nominal 30° for solar zenith angle. The minimum K_d for wavelengths between 443 nm and 665 nm (the visible domain) was used to represent K_d^{tr} in Eq. (32). Further, r_w can be converted to R_{rs} following Lee et al. (2002), and R_{rs}^{pc} was taken as the R_{rs} value corresponding to the wavelength with minimum K_d. Considering the disk is white with $R_T = 0.85$ (Preisendorfer, 1986; Tyler, 1968), r_T is $R_T/\pi \approx 0.27$ sr^{-1}. Also, t^2/n^2 approximates 0.54 for oceanic waters (Austin, 1974; Mobley, 1994), Eq. (32) then becomes

$$Z_{SD} = \frac{1}{2.5\mathrm{Min}(K_d(443,\ 488,\ 532,\ 555,\ 665))}\ln\left(\frac{\left|0.14 - R_{rs}^{pc}\right|}{C_t^r}\right). \tag{33}$$

The threshold contrast (C_t^r) for sighting a white Secchi disk was determined based on the measurements of Blackwell (1946). In that experiment, the difference in brightness (radiance) between the target (B_T) and the background (B_0) was calculated as

$$\Delta B = B_T - B_0. \tag{34}$$

The threshold ΔB was determined at the point when 50% of participants reported loss of sight of the target. Because the sensitivity of human eyes is adaptable to ambient light, ΔB is not a constant but rather changes with the surrounding light intensity. Following the "brightness constancy" concept (Freeman, 1967), the threshold of contrast in reflectance can be calculated as

$$C_t^r = \frac{B_T - B_0}{E_s}, \tag{35}$$

with E_s representing the irradiance of surrounding light. In the experiments, because a majority of the ambient light came from the background screen (which occupies ~5° of the FOV of the human eye), the value of E_s approximated the value of B_0 (where the difference between B_T and B_0 is very small at the detection threshold) (Blackwell, 1946). The resultant C_t^r values are nearly the same for 3–4 orders of magnitude change in the ambient light for a given target size under the photopic vision regime (see Table 8 of Blackwell (1946)), which is consistent with the "brightness constancy" concept. The replacement of E_s by the values of B_0 is appropriate for this experimental setting (Blackwell, 1946), but may not be valid over all observations in the field as ambient light does affect the adaptation of the human eye. The use of B_0 instead of E_s by Blackwell (1946) may also be the reason why researchers followed this approach to evaluate contrast for visual ranging (Eqs. (6) and (9)).

For Secchi disk sighting, where at least a few pixels of the target are required to make a judgment decision on detection, an average (0.013 sr^{-1}) was obtained using the measured C_t^r values for sizes between 3.6 and 9.68 arcmin and for illumination between 10 and 1000 Footlambert (equivalent range is between 34 and 3400 Cd/m^2, for the photopic vision regime). This average is then used for C_t^r in Eq. (33), and a comparison between the measured Z_{SD} and the Eq. (33) calculated Z_{SD} is shown in Fig. 6b.

For this independent Z_{SD} dataset where Z_{SD} is in a range of ~0.1 to 30 m (N = 338, 3 points were excluded as outliers, see Fig. 6b), the mean absolute relative difference between the estimated and measured Z_{SD}, defined as the arithmetic average of $2^*|Z_{SD\text{-}est} - Z_{SD\text{-}mea}|/(Z_{SD\text{-}est} + Z_{SD\text{-}mea})$ from all data pairs, is 18.2%. Linear regression yields a coefficient of determination (R^2) of 0.96, with a slope of 1.04 and intercept of ~0.2 m (see Fig. 6b). Considering that the 18.2% absolute relative difference includes both uncertainties in field-measured Z_{SD} (typically ~10% or more) and uncertainties in K_d derived from non-perfect R_{rs} (Lee et al., 2013), this performance suggests that the new model for Z_{SD} (which includes approximations of $K_d^{pc} = K_d^{tr}$ and $K_T^{tr} = 1.5\,K_d^{tr}$) is excellent. In particular, in such a validation, the model and its parameterization are completely independent from the measurements covering different regions, thus the results indicate plausible interpretation and estimation of Secchi disk depth and the model's applicability for global waters. This agreement in Z_{SD} also indirectly supports the hypothesis that due to the spectrally-selective attenuation by the water body the eye–brain system likely uses a narrow band associated with the maximum contrast for the detection of a Secchi disk.

Furthermore, it is found that the logarithm term on the right side of Eq. (33) is within a narrow range (2.38 ± 0.03) for such a wide range of waters, which indicates that, as a rule of thumb, Secchi disk depth in water approximates

$$Z_{SD} \sim \frac{1}{K_d^{tr}}. \tag{36}$$

Interestingly, this is similar with the penetration depth for ocean color remote sensing (Gordon & Mcluney, 1975).

5. Discussion and conclusions

Given the excellent agreement between the model (together with its parameterization) predictions from the new theory and the independent visibility measurements from a wide range of environments, it is clear that the new theoretical model regarding Secchi disk depth is plausible. This robust performance is further supported through evaluating the diurnally varying Z_{SD} observed in the field (see Fig. 7). Because K_d varies with sun angle (Gordon, 1989; Kirk, 1984; Lee et al., 2005), the new model provides a consistent explanation of diurnal changes in Z_{SD} (assuming no change of water properties), whereas the classical theory could not predict such a variation because c is an IOP and c is significantly larger than K_d. However, it is desired and necessary to carry out more, especially controlled, measurements of Z_{SD}, IOPs, and K_d with changing incident angles for such evaluations. In particular, narrow-band filters should be used to evaluate the sensitivity of human eyes to contrasts in different colors (i.e., wavelengths) in the real aquatic environments together with these measurements.

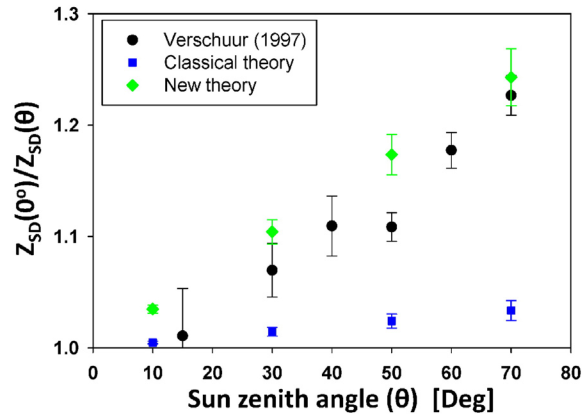

Fig. 7. Diurnal variation of Secchi disk depth. (Black) Ratio of $Z_{SD}(0°)$ to $Z_{SD}(\theta)$ for measurements made in Garner Lake, TN (Verschuur, 1997), with data visually interpreted (average of five persons) from Fig. 3 of Verschuur (1997) and $Z_{SD}(0°)$ extrapolated from observations around 10°–20°. (Blue) Predicted ratio of $Z_{SD}(0°)$ to $Z_{SD}(\theta)$ based on Eq. (10) (the classical theory), which is an average (along with standard deviation) for chlorophyll-a concentration 0.5, 1.0, and 3.0 mg/m^3, respectively. For each chlorophyll-a concentration, the IOPs were simulated following the hyperspectral model of Lee et al. (1998), and a backscattering efficiency of 0.015 was used to convert particle backscattering coefficient to total scattering coefficient. (Green): Predicted ratio of $Z_{SD}(0°)$ to $Z_{SD}(\theta)$ based on Eq. (29) (the new model), also an average (along with standard deviation) for chlorophyll-a concentration as 0.5, 1.0, and 3.0 mg/m^3, respectively. IOPs used in the new theory were the same as those for the classical theory, and spectral K_d was modeled following Lee et al. (2013).

The new theoretical interpretation of Secchi disk depth provides a more generalized view of visual ranging of "large" objects (but within the field-view of a human eye), while the subsequent mechanistic model for Z_{SD} will have profound implications on remote sensing of water transparency and on studies of aquatic environments. First, because Z_{SD} is a function of K_d, analytical remote sensing of water transparency on a global scale via ocean color remote sensing is now possible because spectral K_d is a standard data product of satellite ocean color missions. In contrast, Z_{SD} mainly depends on c in the classical theory, where c is impossible to be analytically derived from passive remote sensing (Gordon, 1993) unless it is highly correlated with K_d. Note that water transparency has direct impact on a wide range of biogeochemical processes (e.g., photosynthesis, photo-oxidation, etc.) and bottom substrates such as coral reefs and sea grasses (Chen, Muller-Kargera, & Hu, 2007; Letelier, Karl, Abbott, & Bidigare, 2004; Sathyendranath & Platt, 1988; Vodacek, Blough, DeGrandpre, Peltzer, & Nelson, 1997; Weeks et al., 2012; Yentsch et al., 2002; Zimmerman, 2006). In the past and present, usually this is done via empirical tuning of regional Z_{SD} algorithms (Chen et al., 2007; Gallegos et al., 2011; Kratzer et al., 2003; Stock, 2015), but there is always a challenge to define the spatial and temporal limitations of such local or regional algorithms. Further, in the past when modern instruments were not widely available for optical measurements of natural waters, Z_{SD} was the standard measurement for a wide range of waters, with a large volume of data collected and archived (Boyce et al., 2012). The availability of such data and the mechanistic model developed here make it possible to derive new and robust remote sensing products to study global changes since the late 1970s. Such a task has been notoriously difficult to accomplish with other data products (e.g., chlorophyll-a concentration) due to the scarcity of measurements in the 1970s and 1980s, and contrary conclusions were sometimes reached from the same satellite ocean color measurements (Antoine, Morel, Gordon, Banzon, & Evans, 2005; Gregg, Casey, & McClain, 2005). Finally, there is a vast warehouse of in-situ data being collected through Citizen Science Projects (e.g., the Secchi Dip-In, http://www.secchidipin.org/index.php/monitoring-methods/; the Secchi APP, http://www1.plymouth.ac.uk/marine/secchidisk/Pages/default.aspx), thus the robust mechanistic model developed here provides a strong base to link these measurements with satellite estimations and the ability to compare the quality of various water bodies.

There have been numerous studies trying to link the attenuation coefficient of the photosynthetically available radiation (K_{PAR}, m^{-1}) with Z_{SD}, from which a wide range of empirical relationships have been reported (Bukata et al., 1988; Effler, 1988; Hojerslev & Aarup, 2002; Holmes, 1970; Padial & M.Thomaz, 2008; Poole & Atkins, 1929; Tyler, 1968). This lack of algorithm uniformity via K_{PAR} is a result of two factors: (1) Visual ranging in water likely measures light in the spectrally transparent window, where K_{PAR} does not provide such information. Actually the contribution of K_d^{tr} to K_{PAR} is secondary compared to the contributions from other wavelengths that have higher attenuation coefficients (e.g., 600–700 nm in oceanic waters; 400–500 nm for coastal turbid waters), and; (2) because K_{PAR} strongly depends on the depth range used for its calculation (Lee, 2009; Megard & Berman, 1989; Morel, 1988), there are large ambiguities in the measured and reported K_{PAR} values. Therefore, to model Z_{SD} of global waters as a function of K_{PAR} is not supported from the radiative transfer point of view.

In conclusion, due to the neglect of the target size and the doubtful use of contrast evaluation for visual judgment by the human eye, the century-old classical underwater visibility theory is found questionable in interpreting Secchi disk depth. The new theory tries to resolve both elements, resulting in a new Law of Contrast Reduction and a new mechanistic model to explain and predict Secchi disk depth, which is further validated and supported using data independently collected from a wide range of aquatic environments. Although the ultimate proof of the new theory regarding ranging of an under-water target by a human eye would require carefully designed field experiments, the mechanistic model developed here is expected to significantly improve the monitoring of water transparency of global waters via ocean color remote sensing and the findings here would expand our understanding of underwater visibility and visual ranging in general.

Acknowledgments

We are in debt to all scientists who provided the valuable field data for community use. Financial support was provided by the National Natural Science Foundation of China (No. 41376177, Shang; No. 41471284, Du) and Ministry of Science and Technology of China (No. 2013BAB04B00, Shang), the National Aeronautic and Space Administration (NASA) (NNX14AK08G, NNX14AQ47A, NNX14AM15G) Ocean Biology and Biogeochemistry and Water and Energy Cycle Programs (Lee, Hu), the National Oceanic and Atmospheric Administration (NOAA) (DG-133E-12-SE-1931) JPSS VIIRS Ocean Color Cal/Val Project (Lee, Hu), Office of Naval Research (PE 0602435N, Hou, Weidemann), and the University of Massachusetts Boston (P20120000019675). Comments and suggestions by Curt Mobley and Ron Zaneveld greatly improved this manuscript.

Appendix A. An illustration of the relationship between K_d^{pc} and K_d^{tr}

Following the radiative transfer theory, it has been found that the depth-averaged diffuse attenuation coefficient of downwelling plane irradiance can be expressed as (Gordon, 1989; Lee et al., 2005)

$$K_d(\lambda) = f(a(\lambda), b_b(\lambda), \theta_S) \tag{A1}$$

with θ_S being the solar zenith angle. a and b_b are the absorption and backscattering coefficients, respectively, and can be expressed as (Mobley, 1994)

$$a(\lambda) = a_w(\lambda) + a_{ph}(\lambda) + a_{dg}(\lambda), \tag{A2}$$

$$b_b(\lambda) = b_{bw}(\lambda) + b_{bp}(\lambda). \tag{A3}$$

Here the subscripts "w, ph, dg" represent water molecules, phytoplankton pigments, and the combination of detrital particles and gelbstoff, respectively; and b_{bp} represents backscattering coefficient of particulates. a_w and b_{bw} spectra are known (Morel, 1974; Pope & Fry, 1997) and considered constants. a_{ph} spectrum in the visible domain (5-nm resolution) can be modeled as a function of $a_{ph}(440)$ (Lee et al., 1998) while $a_{ph}(440)$ can be modeled as a function of [Chl] (Bricaud, Babin, Morel, & Claustre, 1995)

$$a_{ph}(440) = 0.05\,[Chl]^{0.65}. \tag{A4}$$

Spectral a_{dg} can be expressed as an exponential-decay function of wavelength with a spectral slope as 0.015 nm^{-1} (Bricaud, Morel, & Prieur, 1981; Carder, Steward, Harvey, & Ortner, 1989) and $a_{dg}(440)$ was considered equal to $a_{ph}(440)$ in the simulations (Morel, Claustre, Antoine, & Gentili, 2007; Morel & Maritorena, 2001).

Spectral b_{bp} can be modeled as (Gordon & Morel, 1983)

$$b_{bp}(\lambda) = b_{bp}(440)\left(\frac{440}{\lambda}\right), \tag{A5}$$

and $b_{bp}(440)$ was modeled as the following (Gordon & Morel, 1983; Loisel & Morel, 1998) after considering a 1.5% backscattering/scattering ratio

$$b_{bp}(440) = 0.006[Chl]^{0.6}. \tag{A6}$$

a and b_b spectra in the visible domain (5-nm resolution) were then modeled following the above descriptions for [Chl] as 0.03, 0.1, 0.3, 1, 3, 10, and 30 mg/m^3, respectively. We further obtained spectral K_d for $\theta_S = 30°$ from zenith, and obtained K_d^{tr} for each [Chl].

To obtain K_d^{pc} for each [Chl], L_w spectrum was first calculated through Hydrolight (Mobley & Sundman, 2013) for each pair of spectral a and b_b along with the Sun at 30° from zenith and a clear sky (with default atmospheric properties in Hydrolight). The L_w spectrum was then converted to a CIE color following the tristimulus calculations, and a corresponding wavelength was determined for the perceived color in the CIE chromaticity diagram (see Fig. 4 for examples). The value of K_d^{pc} was further sorted based on this wavelength from the spectral K_d for each [Chl], and Fig. 5 shows the relationship between K_d^{pc} and K_d^{tr} from these simulations.

References

Aas, E., Høkedal, J., & Sørensen, K. (2014). Secchi depth in the Oslofjord–Skagerrak area: Theory, experiments and relationships to other quantities. *Ocean Sciences*, *10*, 177–199.

Albert, A., & Mobley, C. D. (2003). An analytical model for subsurface irradiance and remote sensing reflectance in deep and shallow case-2 waters. *Optics Express*, *11*, 2873–2890.

Antoine, D., Morel, A., Gordon, H. R., Banzon, V. F., & Evans, R. H. (2005). Bridging ocean color observations of the 1980s and 2000s in search of long-term trends. *Journal of Geophysical Research*, *110*, C06009 (doi:01029/02004JC002620).

Arnone, R. A., Tucker, S. P., & Hilder, F. A. (1984). Secchi depth atlas of the world coastlines. *Ocean Optics VII, Proc. SPIE 0489*. Monterey, CA: The Society of Photo-Optical Instrumentation Engineers. http://dx.doi.org/10.1117/1112.943305.

Austin, R. W. (1974). Inherent spectral radiance signatures of the ocean surface. In S. W. Duntley (Ed.), *Ocean Color Analysis* (pp. 1–20). San Diego: Scripps Inst. Oceanogr.

Bartleson, C. J., & Breneman, E. J. (1967). Brightness perception in complex fields. *Journal of the Optical Society of America*, *57*, 953–957.

Binding, C. E., Jerome, J. H., Bukata, R. P., & Booty, W. G. (2007). Trends in water clarity of the lower great lakes from remotely sensed aquatic color. *Journal of Great Lakes Research*, *33*, 828–841.

Blackwell, H. R. (1946). Contrast thresholds of the human eye. *Journal of the Optical Society of America*, *36*, 624–643.

Bowers, T. E., Jugan, L. A., McBride, W. E., Davis-Lunde, K., Weidemann, A. D., Mahoney, K., & Morgan, E. (2000). Project GLOW: Results from in-situ validation of the US NAVY's algorithm to determine underwater horizontal visibility. *Ocean Optics XV* (Monaco).

Boyce, D. G., Lewis, M. R., & Worm, B. (2010). Global phytoplankton decline over the past century. *Nature*, *466*, 591–596 (doi:510.1038/nature09268).

Boyce, D. G., Lewis, M., & Worm, B. (2012). Integrating global chlorophyll data from 1890 to 2010. *Limnology and Oceanography: Methods*, *10*, 840–852.

Bricaud, A., Babin, M., Morel, A., & Claustre, H. (1995). Variability in the chlorophyll-specific absorption coefficients of natural phytoplankton: Analysis and parameterization. *Journal of Geophysical Research*, *100*, 13321–13332.

Bricaud, A., Morel, A., & Prieur, L. (1981). Absorption by dissolved organic matter of the sea (yellow substance) in the UV and visible domains. *Limnology and Oceanography*, *26*, 43–53.

Bukata, R. P., Jerome, J. H., & Bruton, J. E. (1988). Relationships among Secchi disk depth, beam attenuation coefficient, and irradiance attenuation coefficient for Great Lakes waters. *Journal of Great Lakes Research*, *14*, 347–355.

Carder, K. L., Steward, R. G., Harvey, G. R., & Ortner, P. B. (1989). Marine humic and fulvic acids: Their effects on remote sensing of ocean chlorophyll. *Limnology and Oceanography*, *34*, 68–81.

Carlson, R. E. (1977). A trophic state index for lakes. *Limnology and Oceanography*, *22*, 361–369.

Chen, Z., Muller-Kargera, F. E., & Hu, C. (2007). Remote sensing of water clarity in Tampa Bay. *Remote Sensing of Environment*, *109*, 249–259.

Clark, R. N. (1990). *Visual Astronomy of the Deep Sky*. Cambridge: Cambridge University Press and Sky Publishing.

Curcio, C. A., Sloan, K. R., Kalina, R. E., & Hendrickson, A. E. (1990). Human photoreceptor topography. *Journal of Comparative Neurology*, *292*, 497–523.

Davies-Colley, R. J., & Vant, W. N. (1988). Estimation of optical properties of water from Secchi disk depths. *Water Resources Bulletin*, *24*, 1329–1335.

Devlin, M. J., Barry, J., Mills, D. K., Gowen, R. J., Foden, J., Sivyer, D., & Tett, P. (2008). Relationships between suspended particulate material, light attenuation and Secchi depth in UK marine waters. *Estuarine, Coastal and Shelf Science*, *79*, 429–439.

Doron, M., Babin, M., Hembise, O., Mangin, A., & Garnesson, P. (2011). Ocean transparency from space: Validation of algorithms using MERIS, MODIS and SeaWiFS data. *Remote Sensing of Environment*, *115*, 2986–3001.

Duntley, S. Q. (1952). The visibility of submerged objects. *Visibility Lab., Mass. Inst. Tech* (pp. 74). San Diego: Scripps Institution of Oceanography.

Effler, S. (1988). Secchi disc transparency and turbidity. *Journal of Environmental Engineering*, *114*, 1436–1447.

Freeman, R. B. (1967). Contrast interpretation of brightness constancy. *Psychological Bulletin*, *67*, 165–187.

Gallegos, C. L., Werdell, P. J., & McClain, C. R. (2011). Long-term changes in light scattering in Chesapeake Bay inferred from Secchi depth, light attenuation, and remote sensing measurements. *Journal of Geophysical Research*, *116*http://dx.doi.org/10.1029/2011JC007160.

Gordon, H. R. (1978). Some relationships between Secchi depth and inherent optical properties of natural waters. *Applied Optics*, *17*, 3341–3343.

Gordon, H. R. (1989). Can the Lambert–Beer law be applied to the diffuse attenuation coefficient of ocean water? *Limnology and Oceanography*, *34*, 1389–1409.

Gordon, H. R. (1993). Sensitivity of radiative transfer to small-angle scattering in the ocean: Quantitative assessment. *Applied Optics*, *32*, 7505–7511.

Gordon, H. R., & Mcluney, W. R. (1975). Estimation of the depth of sunlight penetration in the sea for remote sensing. *Applied Optics*, *14*, 413–416.

Gordon, H. R., & Morel, A. (1983). *Remote assessment of ocean color for interpretation of satellite visible imagery: A review*. New York: Springer-Verlag.

Gregg, W. W., Casey, N. W., & McClain, C. R. (2005). Recent trends in global ocean chlorophyll. *Geophysical Research Letters*, *32*, L03606 (doi:03610.01029/02004GL021808).

Højerslev, N. K. (1986). Visibility of the sea with special reference to the Secchi disc. In M.A. Blizard (Ed.), *Ocean Optics VIII, SPIE 637* (pp. 294–305).

Hojerslev, N. K., & Aarup, T. (2002). Optical measurements on the Louisiana Shelf off the Mississippi River. *Estuarine, Coastal and Shelf Science*, *55*, 599–611.

Holmes, R. W. (1970). The Secchi disk in turbid coastal waters. *Limnology and Oceanography*, *15*, 688–694.

Hou, W., Lee, Z. -P., & Weidemann, A. D. (2007). Why does the Secchi disk disappear? An imaging perspective. *Optics Express*, *15*, 2791–2802.

Judd, D. B., & Wyszecki, G. (1975). *Color in Business, Science and Industry*. New York: Wiley-Interscience.

Kirk, J. T. O. (1984). Dependence of relationship between inherent and apparent optical properties of water on solar altitude. *Limnology and Oceanography*, *29*, 350–356.

Kirk, J. T. O. (1991). Volume scattering function, average cosines, and the underwater light field. *Limnology and Oceanography*, *36*, 455–467.

Kirk, J. T. O. (1994). *Light & Photosynthesis in Aquatic Ecosystems*. Cambridge: University Press.

Kratzer, S., Håkansson, B., & Sahlin, C. (2003). Assessing Secchi and photic zone depth in the Baltic Sea from satellite data. *Ambio*, *32*, 577–585.

Lee, Z. P. (2009). KPAR: An optical property associated with ambiguous values. *Journal of Lake Science*, *21*, 159–164.

Lee, Z. P., Carder, K. L., & Arnone, R. (2002). Deriving inherent optical properties from water color: A multi-band quasi-analytical algorithm for optically deep waters. *Applied Optics*, *41*, 5755–5772.

Lee, Z. P., Carder, K. L., Hawes, S. K., Steward, R. G., Peacock, T. G., & Davis, C. O. (1994). A model for interpretation of hyperspectral remote sensing reflectance. *Applied Optics*, *33*, 5721–5732.

Lee, Z. P., Carder, K. L., Mobley, C. D., Steward, R. G., & Patch, J. S. (1998). Hyperspectral remote sensing for shallow waters. 1. A semianalytical model. *Applied Optics*, *37*, 6329–6338.

Lee, Z. P., Du, K. P., & Arnone, R. (2005). A model for the diffuse attenuation coefficient of downwelling irradiance. *Journal of Geophysical Research*, *110*http://dx.doi.org/10.1029/2004JC002275.

Lee, Z. P., Hu, C., Shang, S., Du, K., Lewis, M., Arnone, R., & Brewin, R. (2013). Penetration of UV – Visible solar light in the global oceans: Insights from ocean color remote sensing. *Journal of Geophysical Research*, *118*, 4241–4255 (doi:4210.1002/jgrc.20308).

Letelier, R. M., Karl, D. M., Abbott, M. R., & Bidigare, R. R. (2004). Light driven seasonal patterns of chlorophyll and nitrate in the lower euphotic zone of the North Pacific Subtropical Gyre. *Limnology and Oceanography*, *49*, 508–519.

Lewis, M. R., Kuring, N., & Yentsch, C. (1988). Global patterns of ocean transparency: Implications for the new production of the open ocean. *Journal of Geophysical Research*, *93*, 6847–6856.

Loisel, H., & Morel, A. (1998). Light scattering and chlorophyll concentration in Case 1 waters: A reexamination. *Limnology and Oceanography*, *43*, 847–858.

Lyzenga, D. R. (1981). Remote sensing of bottom reflectance and water attenuation parameters in shallow water using aircraft and Landsat data. *International Journal of Remote Sensing*, *2*, 71–82.

Megard, R. O., & Berman, T. (1989). Effects of algae on the Secchi transparency of the southeastern Mediterranean Sea. *Limnology and Oceanography*, *34*, 1640–1655.

Middleton, W. E. K. (1952). *Vision Through the Atmosphere*. Toronto: University of Toronto Press.

Mobley, C. D. (1994). *Light and Water: Radiative Transfer in Natural Waters*. New York: Academic Press.

Mobley, C. D. (1999). Estimation of the remote-sensing reflectance from above-surface measurements. *Applied Optics*, *38*, 7442–7455.

Mobley, C. D., & Sundman, L. K. (2013). *HydroLight 5.2 User's Guide*. Bellevue, Washington: Sequoia Scientific, Inc.

Morel, A. (1974). Optical properties of pure water and pure sea water. In N. G. Jerlov, & E. S. Nielsen (Eds.), *Optical Aspects of Oceanography* (pp. 1–24). New York: Academic.

Morel, A. (1988). Optical modeling of the upper ocean in relation to its biogenous matter content (Case I waters). *Journal of Geophysical Research*, *93*, 10749–10768.

Morel, A., Claustre, H., Antoine, D., & Gentili, B. (2007). Natural variability of bio-optical properties in Case 1 waters: attenuation and reflectance within the visible and near-UV spectral domains, as observed in South Pacific and Mediterranean waters. *Biogeosciences*, *4*, 913–925.

Morel, A., Huot, Y., Gentili, B., Werdell, P. J., Hooker, S. B., & Franz, B. A. (2007). Examining the consistency of products derived from various ocean color sensors in open ocean (Case 1) waters in the perspective of a multi-sensor approach. *Remote Sensing of Environment*, *111*, 69–88.

Morel, A., & Maritorena, S. (2001). Bio-optical properties of oceanic waters: A reappraisal. *Journal of Geophysical Research*, *106*, 7163–7180.

Padial, A. A., & M.Thomaz, S. (2008). Prediction of the light attenuation coefficient through the Secchi disk depth: Empirical modeling in two large Neotropical ecosystems. *Limnology*, *9*, 143–151.

Philpot, W. D. (1989). Bathymetric mapping with passive multispectral imagery. *Applied Optics*, *28*, 1569–1578.

Poole, H. H., & Atkins, W. R. G. (1929). Photo-electric measurements of submarine illumination throughout the year. *Journal of the Marine Biological Association of the United Kingdom*, *16*, 297–324.

Pope, R., & Fry, E. (1997). Absorption spectrum (380–700 nm) of pure waters: II. Integrating cavity measurements. *Applied Optics*, *36*, 8710–8723.

Preisendorfer, R. W. (1976). *Hydrologic Optics vol. 1: Introduction*. Springfield: National Technical Information Service (Also available on CD, Office of Naval Research).

Preisendorfer, R. W. (1986). Secchi disk science: Visual optics of natural waters. *Limnology and Oceanography*, *31*, 909–926.

Sathyendranath, S., & Platt, T. (1988). The spectral irradiance field at the surface and in the interior of the ocean: A model for applications in oceanography and remote sensing. *Journal of Geophysical Research*, *93*, 9270–9280.

Shang, S. L., Dong, Q., Lee, Z. P., Li, Y., Xie, Y. S., & Behrenfeld, M. J. (2011). MODIS observed phytoplankton dynamics in the Taiwan strait: An absorption-based analysis. *Biogeosciences*, *8*, 841–850.

Stock, A. (2015). Satellite mapping of Baltic Sea Secchi depth with multiple regressionmodels. *International Journal of Applied Earth Observation and Geoinformation*, *40*, 55–64.

Tyler, J. E. (1968). The Secchi disc. *Limnology and Oceanography*, *13*, 1–6.

Verschuur, G. L. (1997). Transparency measurements in Garner Lake, Tennessee: the relationship between Secchi depth and solar altitude and a suggestion for normalization of Secchi depth data. *Journal Lake and Reservoir Management*, *13*, 142–153.

Vodacek, A., Blough, N., DeGrandpre, M., Peltzer, E., & Nelson, R. (1997). Seasonal variation of CDOM and DOC in the Middle Atlantic Bight: Terrestrial inputs and photooxidation. *Limnology and Oceanography*, *42*, 674–686.

Voss, K. J., Mobley, C. D., Sundman, L. K., Ivey, J. E., & Mazel, C. H. (2003). The spectral upwelling radiance distribution in optically shallow waters. *Limnology and Oceanography*, *48*, 364–373.

Weeks, S., Werdell, J., Schaffelke, B., Canto, M., Lee, Z. -P., Wilding, J., & Feldman, G. (2012). Satellite-derived photic depth on the great barrier reef: Spatio-temporal patterns of water clarity. *Remote Sensing*, *4*, 3781–3795 (doi:3710.3390/rs4123781).

Wells, W. H. (1973a). Factors affecting long range vision. In P. Halley (Ed.), *Optics of the Sea: Interface and In-water Transmission and Imaging* (pp. 4.1.1–4.1.10). London, UK: Technical Editing and Reproduction Ltd.

Wells, W. H. (1973b). Theory of small angle scattering. In P. Halley (Ed.), *Optics of the Sea: Interface and In-water Transmission and Imaging* (pp. 3.3.1–3.3.17). London, UK: Technical Editing and Reproduction Ltd.

Wernand, M. R. (2010). On the history of the Secchi disc. *Journal European Optical Society — Rapid Publications*, *5*, 10013s.

Yentsch, C. S., Yentsch, C. M., Cullen, J. J., Lapointe, B., Phinney, D. A., & Yentsch, S. W. (2002). Sunlight and water transparency: Cornerstones in coral research. *Journal of Experimental Marine Biology and Ecology*, *268*, 171–183.

Zaneveld, J. R. V. (1995). A theoretical derivation of the dependence of the remotely sensed reflectance of the ocean on the inherent optical properties. *Journal of Geophysical Research*, *100*, 13135–13142.

Zaneveld, J. R., & Pegau, W. S. (2003). Robust underwater visibility parameter. *Optics Express*, *11*, 2997–3009.

Zhang, J. S., Wei, G. M., Lin, G., & Shang, S. L. (2014). Evaluation of the applicability of an IOP-based algorithm to derive Secchi depth. *Journal of Xiamen University (Natural Science)*, *53*http://dx.doi.org/10.6043/j.issn.0438-0479.2014.6004.6001.

Zimmerman, R. C. (2006). Light and photosynthesis in seagrass meadows. In A. W. D. Larkum, R. J. Orth, & C. M. Duarte (Eds.), *Seagrasses: Biology, Ecology and Conservation* (pp. 303–321). Dordrechet, The Netherlands: Springer.